



A HIGH INTENSITY RF BEAM

Joseph Lach

May 22, 1974

The last year has seen a significant advancement in the state of the art of the radio-frequency separator technology and it is the aim of this note to reassess the potentials of such devices for NAL in the light of these developments.

Recent Developments

In 1972 NAL supported a development program at Brookhaven National Laboratory (BNL) aimed at producing a seven cell prototype of a superconducting rf separator at X-band (8.7 GHz). Last year the BNL group successfully completed such a structure and measured its properties. Their results are described in Ref. 1. From these studies it was then possible to specify, for the first time, a set of realistic design parameters for an rf separator which could be then used in a beam design. The design parameter table, taken from Ref. 1, is reproduced here as Table I. The purpose of this note is to investigate the properties of an rf beam which could be built using deflectors with these parameters.

The Deflectors

Only a few of the parameters of Table I are relevant

-2-

for the optical design of the beam. These are the operating frequency 8.665 GHz, the diameter of the deflector aperture, 13.3 mm, the length of the deflector and the transverse momentum, \underline{p}_\perp , imparted by the deflectors. We will consider two possible lengths, A and B. The former will be 2.29 m long and will have $\underline{p}_\perp = 10.8$ MeV/c; the latter 3.43 m and $\underline{p}_\perp = 16$ MeV/c. The deflector material is high purity Niobium and is designed to operate at 1.5°K. The reader is referred to Ref. 1 for more details of the deflecting structure.

Scaling a Previous Design

A rather complete design was made for an X-band rf beam² in 1965 and although the deflection parameters must be modified the same basic three deflector design can be used. In fact we will simply scale the graphs showing the momentum regions where separation is possible to the frequency and beam length of interest here. We will assume a beam with the following parameters and component lengths.

- 250 m Momentum analysis section, re-imaging section, and momentum recombination section.
- 357 m Separation between deflector 1 and deflector 2.
- 643 m Separation between deflector 2 and deflector 3.
- 250 m Stopper section, second momentum analysis section, purification section, shaping section.

-3-

The above represents a three deflector beam with the total lengths of the deflector sections of 1000 m and a total beam length of 1500 m. No detailed optical design has been done but from previous experience the parameters seem reasonable and will be sufficient for us to estimate fluxes, regions of separation, etc. In our subsequent discussion we will assume that our beam consists of three components: pions, kaons, and protons (or antiprotons).

Momentum Regions of Separation

We can represent the momentum regions where separation is practical in a convenient way if we plot the difference in average angular deflection (actually the difference in the magnitudes) between any two particle types of interest when we have adjusted the deflector phases to cancel the deflection of the third particle. This can be done if we just use two of our three deflectors; here we will use the outer two and turn the middle one off. We can then consider a number of cases.

1. Adjust phase so that the proton net deflections, $A_p = 0$. We then plot the difference in the amplitudes of the pions, $|A_\pi|$ and the kaons, $|A_k|$. This is shown in Fig. 1. The units are such that the deflection from a single deflector, α_D , is one. Hence if the natural angular divergence of the beam in the first deflector, α_V , is equal to α_D

-4-

then good separation is achieved for momentum regions where the $\left| |A_{\pi}| - |A_k| \right| > 1$. If this ratio $\alpha_V/\alpha_D \equiv \eta = 0.5$ then good separation can be achieved whenever $\left| |A_{\pi}| - |A_k| \right| > 0.5$ and so on. From Fig. 1 we see that there is a region of easy π separation at about 95 GeV/c and then a broad region of K separation just above 100 GeV/c.

2. Adjust phase so that the pion net deflections $A_{\pi} = 0$. We plot $|A_p| - |A_k|$ in Fig. 2. Here we see the clean kaon separation region near 160 GeV/c.
3. Adjust phase so that kaon net deflection $A_k = 0$. We plot $|A_{\pi}| - |A_p|$ in Fig. 3. Here we see a sharp region of clean pion separation just under 100 GeV/c and then a broad region of proton separation near 160 GeV/c.

If all three deflectors are used it is possible to determine a set of phases and deflector amplitudes which give us zero net deflection for two particle types and in general a finite deflection for the third.² As in the previous two deflector case the units are such that the deflection from a single deflector is one. Figures 4 - 6 show the resultant deflection amplitudes for pions, kaons and protons as a function of momentum when the deflection amplitude of both unwanted particles have been set to zero.

The condition described in the previous paragraph of using three deflectors and adjusting the deflector parameters to zero net deflection for both unwanted particles is a very stringent condition. The practice with existing rf beams is that one can relax some of these conditions and get adequate separation at momentum ~30% higher than one would expect from the previous discussion. This means that this beam would be adequate for pion separation up to momentum of about 200 GeV/c. Certain trade offs of purity for intensity can be achieved and these momentum limits can be pushed higher. One could certainly go up to 200 GeV/c to suppress protons in order to get an enriched π^+ beam if one did not worry about the K^+ contamination. In general one can say that regions of useful particle separation will extend throughout the momentum region of 100-200 GeV/c.

Deflector Acceptance and Beam Solid Angle

Given the properties of the deflectors we would now like to investigate what limitations this puts on the solid angle acceptance hence flux of the beam. It can be shown³ that the maximum vertical and horizontal angular acceptance, α_V and α_H at the target is given by

$$\alpha_V = \frac{\alpha_D}{\epsilon_V \eta} \left\{ s - \ell \alpha_D \left(2 + \frac{1}{\eta} \right) \right\}$$

$$\alpha_H = \frac{s^2}{4t_H \ell}$$

where α_D = angular acceptance (1/2 angle) of single deflector

a = aperture of deflector

ℓ = length of deflector

$s = 8^{-1/2} a = 1/2$ side of inscribed square

t_V = target 1/2 height

t_H = target 1/2 width

m_V = verticle magnification from target to deflector

$$\eta = \frac{\alpha_D m_V}{\alpha_V}$$

Once α_V and α_H are determined we can write the solid angle acceptance Ω as

$$\Omega = \pi \alpha_V \alpha_H$$

We have assumed that the separation plane is the verticle plane. Fig. 7 is a plot of Ω as a function of momentum for the deflector lengths A and B. Also plotted is Ω if the rf were turned off but with the deflectors in place; i.e. the acceptance limitation of the unpowered deflectors. In these computations we have assumed $\eta = 1$ and $t_H = t_V = 0.5$ mm.

-7-

We see from Fig. 7 that the deflectors allow for very large solid angle acceptances. In fact for beams in the 100 - 200 GeV/c range the limitation would not be the deflectors but the aperture of the beam transport magnets. The very important conclusion is that to a first approximation the deflectors we have chosen do not limit the solid angle acceptance of our beam.

Production Cross Sections

In our flux estimates we will use the Wang⁴ cross section parameterization which has the beauty that it can be written in closed form and easily integrated. We will integrate the Wang distribution out to some angle centered about the forward direction and for the solid angle corresponding to this angle plot $\frac{pdN}{dp}$ the number of produced π^- per $\Delta p/p$ per interacting proton as a function of secondary momentum. This is shown in Fig. 8. Here we have assumed 300 GeV protons incident on a light target and an azimuthally symmetric solid angle bite centered on zero degrees. We note that the flux increases rapidly as a function of solid angle for small values of solid angle and then reaches an asymptotic value indicated on the figure for each momentum. Thus little flux is to be gained by going to very large acceptances. Figures 9 and 10 show similar graphs for incident energies of 500 and 1000 GeV respectively. The effect is even more pronounced here.

Decay Losses.

For beams of kilometer lengths losses due to the decay of the particles can be substantial and are in fact what puts the lower momentum limit to our K fluxes. This can be seen in Fig. 11 where we plot the fraction of K^\pm surviving versus length for various momenta. For our 1.5Km beam at 100 GeV/c only 13.6% survive to the end, at 200 GeV/c this increases to 36.8%. Although these losses are substantial we are still left with very intense kaon beams. Figure 12 shows a similar loss plot for π^\pm . Here the losses are not serious for our 1.5Km beam.

Fluxes.

We will use the π^- and π^+ fluxes as computed from the Wang⁴ formula and the recently measured particle production ratios⁵ to estimate fluxes for the other particles. Figure 13 shows these ratios using a Beryllium target viewed at 3.6 mr. Here X is the ratio of laboratory secondary momenta to the incident momentum and we have assumed that the K/π , \bar{P}/π^- and p/π^+ ratios depend only on X and are given by the measurements of Ref. 5.

From Fig. 7 we see that a reasonable solid angle for our separated beam is 5 μ sr. This is a very large solid angle beam by NAL standards and will probably require building of new high quality optical components.

We are now able to compute our secondary fluxes at the end of the beam line with the following assumptions.

Beryllium Target

$1 \cdot 10^{13}$ interacting protons per pulse.

a solid angle of 5 μ sr centered at zero degrees.

a momentum bite of 2%.

a 50% stopper loss.

Decay losses for a 1.5Km beam line.

Figures 14 - 16 show the resultant fluxes for 300, 500, and 1000 GeV incident protons. One sees that the fluxes are very large indeed. One also sees that very substantial gains are made for secondary momentum of 100 - 200 GeV/c by using primary protons of 500 or 1000 GeV.

Open Questions and Some Partial Answers.

Targeting: We have assumed that $1 \cdot 10^{13}$ protons can be interacted in a target of $1 \times 1 \text{ mm.}^2$ The accelerator beam emittance is in principle good enough to do this and we are getting more experience in stabilizing the external beam to hit small targets. Target heating problems are severe. For ease in cooling, the target could be a horizontal ribbon so that it is well defined in the separation plane; it would probably be sufficient to let the beam spot itself define

-10-

the horizontal target extent.

Optics: We are speaking of a large solid angle beam as measured by present NAL secondary beam acceptances. This will certainly mean the use of high aperture quadrupoles and bending magnets (4" or 8"?) as well as magnets of good optical properties. Recall that angles in the deflector sections must be defined to better than 0.05 mr. The magnifications from target to deflector are between five and ten, not nearly as difficult as in Ref. 2, but still challenging. We would also like this beam to transport a large momentum bite. A momentum bite of 2% is thought to be attainable, one might even do a little better than that. The optical problems of such a beam are difficult but look realizable with a careful and thorough design. No such detailed design has yet been undertaken.

Anisochronism: There will exist a rf phase spread of the beam due to the fact that we will have a finite momentum bite.² To keep the image of the unwanted particles from smearing into the wanted particles this phase spread should be kept to about 0.1 radius. This is only serious when we are trying to reject protons since it is the protons which will have the largest spread in velocity for a given momentum bite. This condition limits the useful momentum acceptance of the beam to about 2% at 100 GeV/c. It is not serious at higher momenta.

-11-

Muons: The problem of muons within the beam phase space, mostly resulting from pion decays in the interdeflector regions, is not too serious but muons in the general downstream area of the beam have to be carefully studied. This could be a limitation for certain experiments.

The Deflectors: A workable deflector design has been described¹ but it is probably not yet optimized for our applications. For example it may be possible to increase the aperture of the deflectors⁶. This would be useful not because of the increased acceptance but because it would then be possible to operate at higher frequencies with the associated scaling down of the aperture. The aperture limit is probably set by the purely technical requirement that the internal electron beam welds must be machined from the inside and the aperture must be big enough to allow a cutting tool to enter the cell. So an optimization of the deflector design which would allow for larger apertures (at a given frequency) would allow us to operate at higher frequencies and hence higher momenta. Many problems associated with the deflectors have not yet been discussed such as phasing of the deflectors, tuning of the frequencies and pressure stabilization. Again none seem insurmountable but all are state of the art items which require careful, thorough and creative engineering.

Location and Configuration: This major new beam line is about 1.5Km long and would require a new targeting area. The most

-12-

natural place for this would be near the so called "Q stub" and, in fact, this should be considered as a candidate for the Q area. Configured in this way the beam line would run nearly parallel to the neutrino area and to the east of it. It would be practical to kick out a small amount of beam for the bubble chambers. This parasitic bubble chamber operation was incorporated into the design of Ref. 2 and should be done here also. Besides the kicker for the bubble chamber beams a switch capable of delivering beam to either of two experimental set ups should also be made an integral part of the design.

Schedules and Cost

At this time NAL has the technical expertise to build all of the components of this beam except for the separators themselves. The feasibility of the deflectors was demonstrated for us by the BNL group but if actual structures are to be built they should be done at NAL. The next step would be the construction of a 1 m section. This could probably be realized 18 - 24 months after a NAL separator group were constituted. With proper priorities and a well organized deliberate effort this beam could be operational in 2 1/2 - 3 years after the project was initiated. No detailed cost estimates have been made but it is expected that the complete project would be in the range of 5 - 10 million dollars.

-13-

Conclusion

We propose a new experimental area whose major facility will be a high intensity spatially separated beams of π^{\pm} , K^{\pm} and \bar{P} . Within the last year the technical feasibility of the major components has been demonstrated. This beam would provide fluxes of the above secondary particles two to three orders of magnitude higher than previously available and open up a new region of particle physics. Some of the physics potentials of this beam are discussed in another note.⁷

This document is intended to open the discussion as to whether the physics potential of this device is worth the cost of construction. This is the overriding consideration which must enter into the decision to construct this device.

Acknowledgements

During the writing of this report I received a paper from H. Lengeler of the Karlsruhe group who points out the possibility of X-band superconducting separated beams for CERN. Since W. Bauer of the Karlsruhe group worked at BNL on the NAL sponsored X-band structure the very valuable free interchange of ideas and people has already benefited the field. I would also like to thank T. Toohig for checking some of my calculations and many useful discussions.

REFERENCES

- ¹J. Aggus, W. Bauer, S. Giordano, H. Hahn and H. J. Halama
BNL 18292 (1973).
- ²J. Lach UCID-10179, also in 200 BeV Accelerator; Studies on
Experimental Use Vol. 1, p. 190 (1966).
- ³J. Lach NAL TM-202 (1970).
- ⁴C. L. Wang, BNL 18798 (1974).
- ⁵W. F. Baker et al., NAL-Pub 74/13 Exp (Submitted to Phys.
Rev. Letters).
- ⁶W. Bauer BNL 17768 (1973).
- ⁷J. Lach et al. TM-494.
- ⁸H. Lengeler, Karlsruhe Institut fur Experimentelle
Kernphysik Interner Bericht NR 74-34 Sep (1974).

TABLE I

Design parameters for a multiperiodic π -mode-like X-band deflecting cavity

Frequency, (GHz)	8.665	
Cell length, (mm)	17.3	
Iris thickness, (mm)	6.7	
Iris hole diameter, (mm)	13.3	
Magnetic field ration H_p/E_o , (G/MV m ⁻¹)	107	
Electric field ratio E_p/E_o	3.63	
Peak magnetic field on iris H_p , (G)	500	
Peak electric field on iris E_p , (MV/m)	17	
Equivalent deflecting field E_o , (MV/m)	4.7	
Shunt Impedance/Q, (Ω /m)	4730	
Improvement factor	5×10^4	
Shunt impedance, (M Ω /m)	2.13×10^6	
Number of sections	5	7
Total length, (m)	2.29	3.43
Number of cells, middle section	3 x 33	5 x 33
Number of cells, end sections	2 x 16½	2 x 16½
Transverse momentum per cavity, (MeV/c)	10.8	16
rf power loss per cavity (W)	24	36

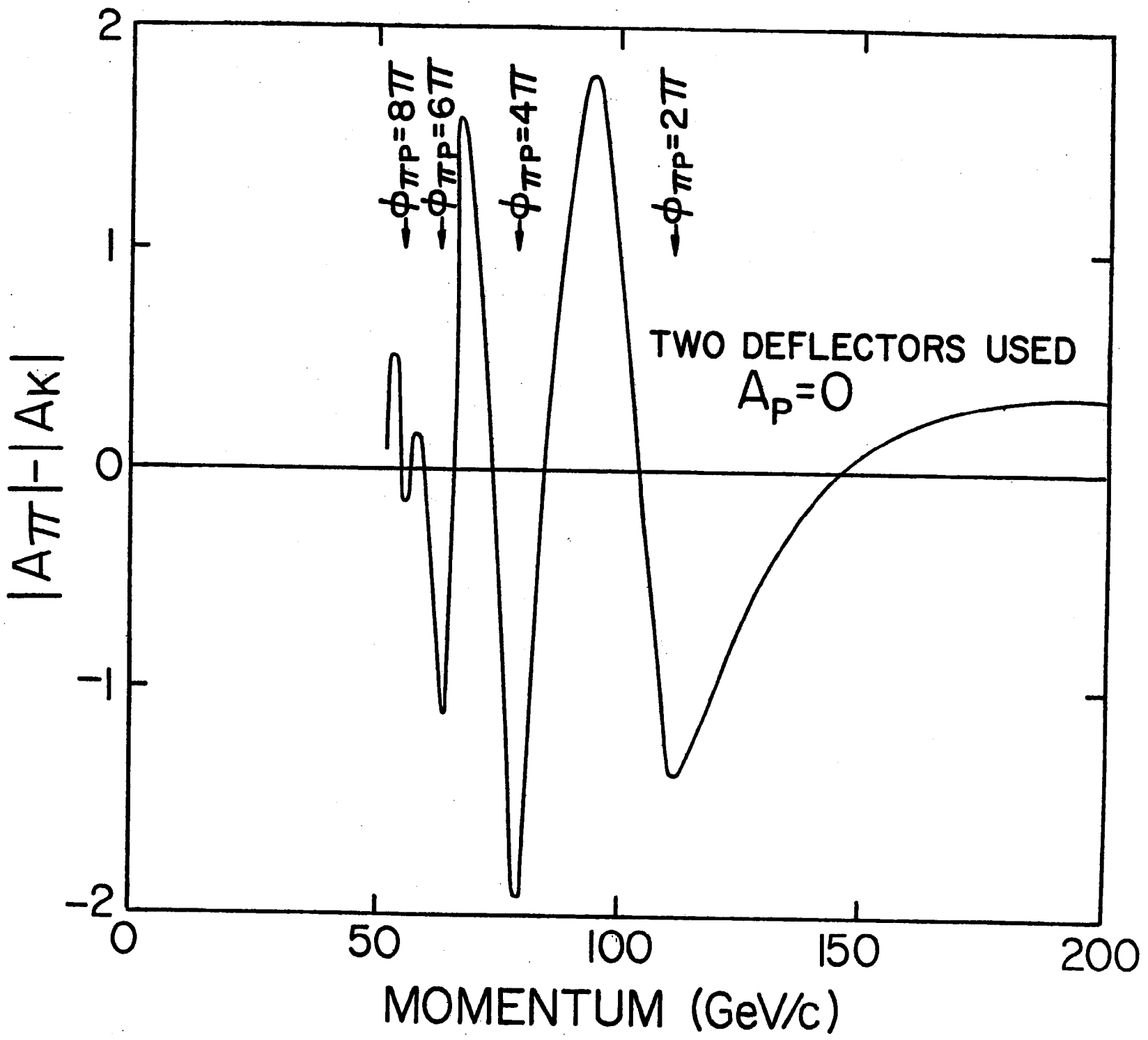


Figure 1

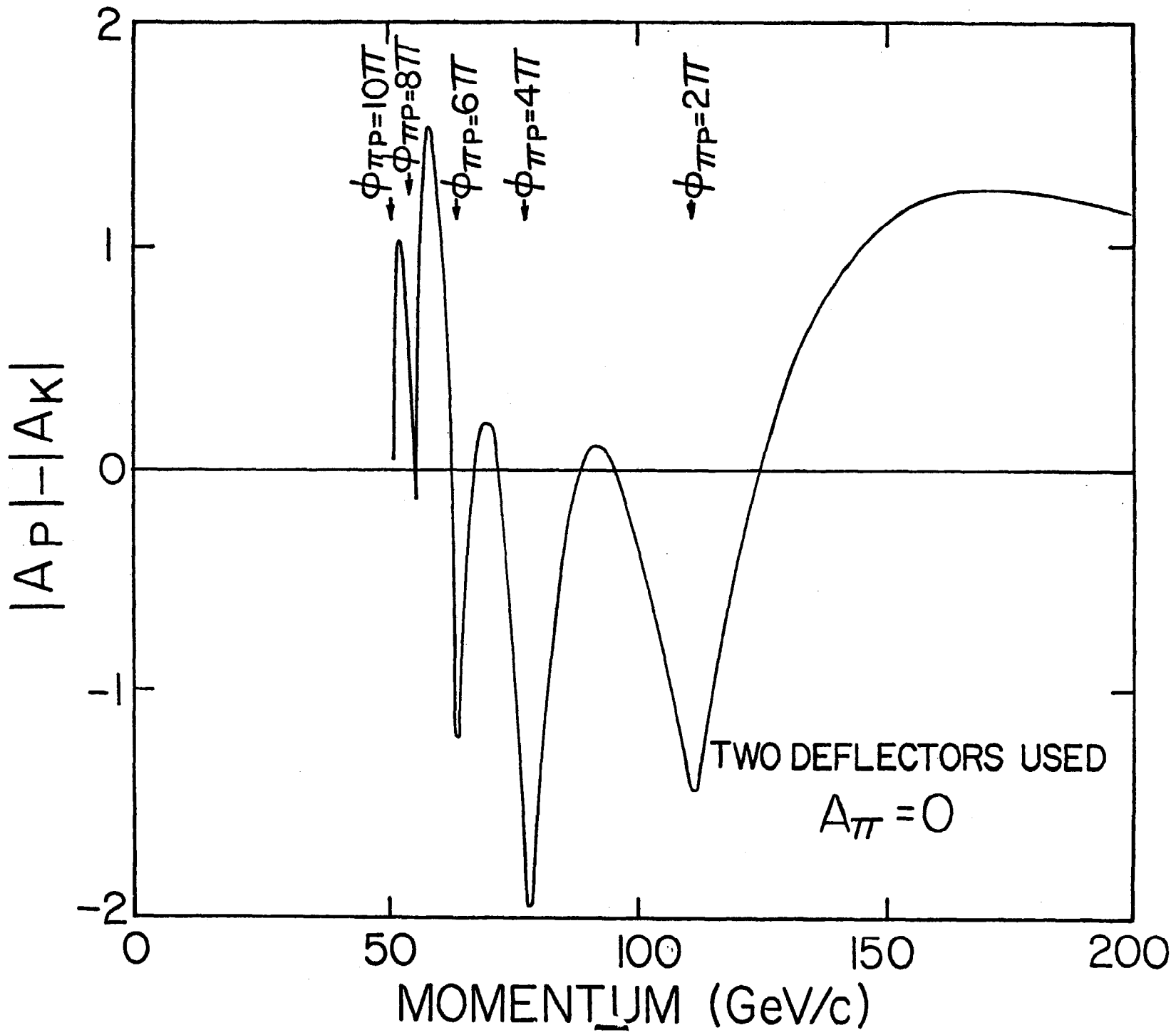


Figure 2

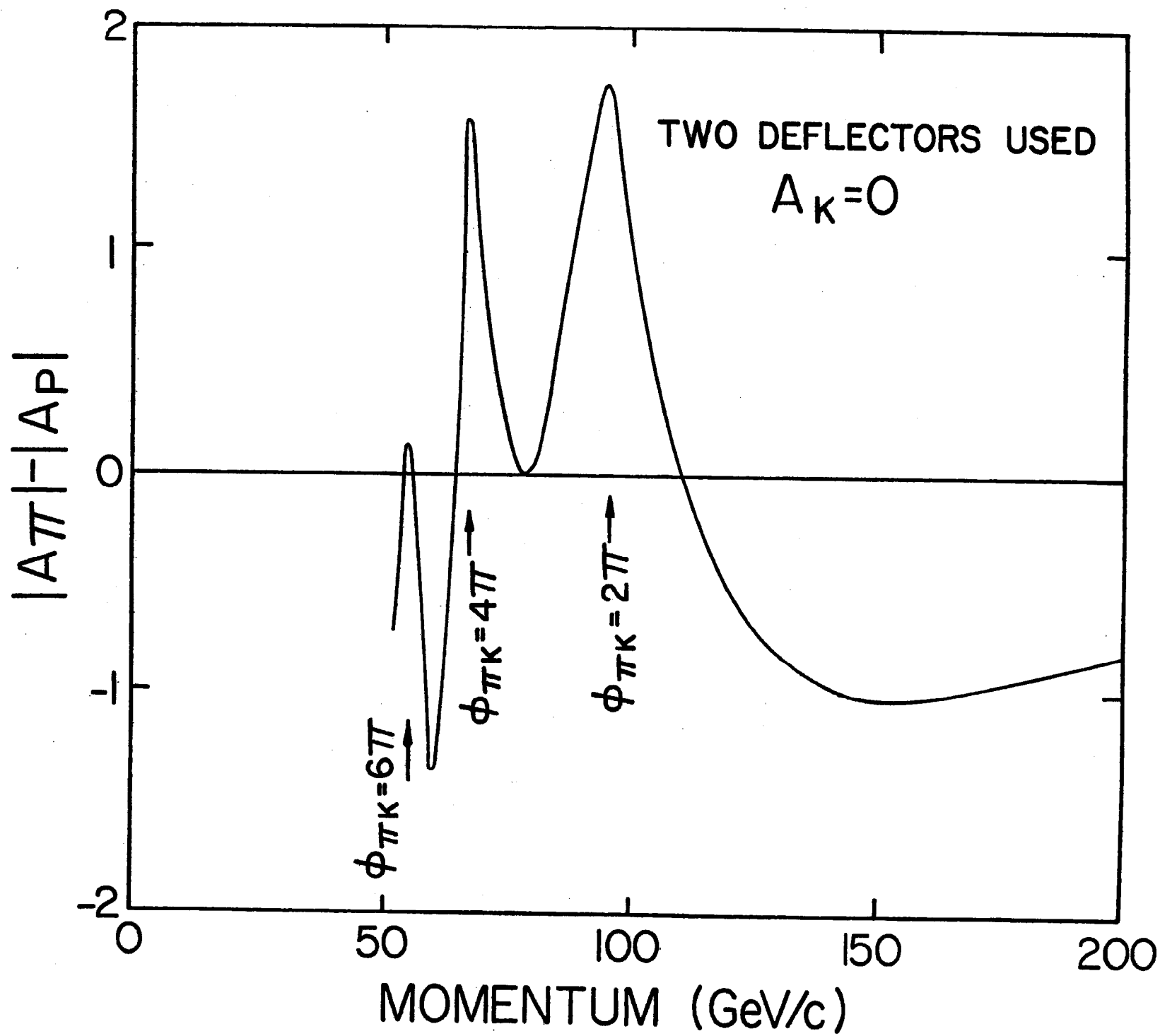
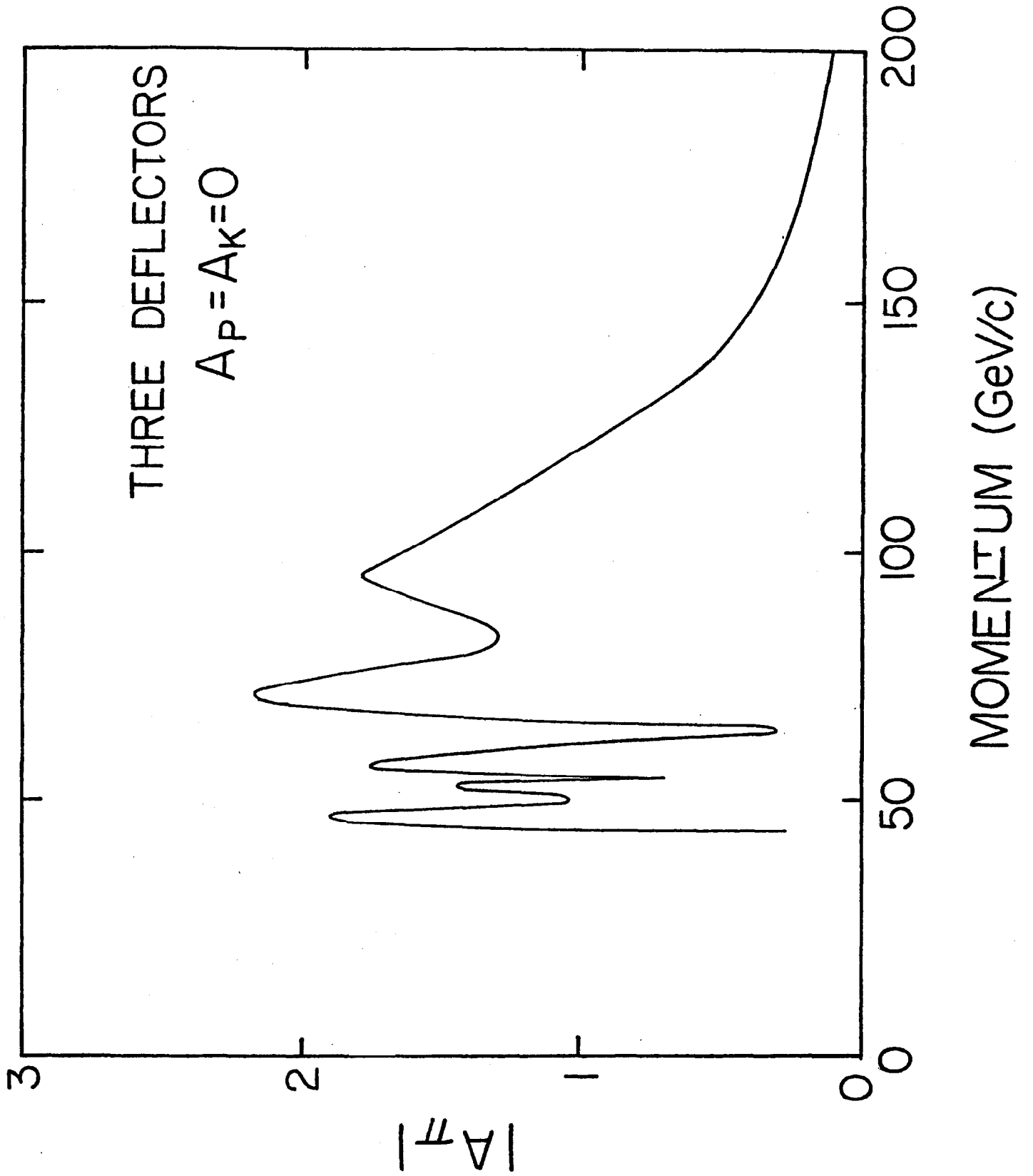
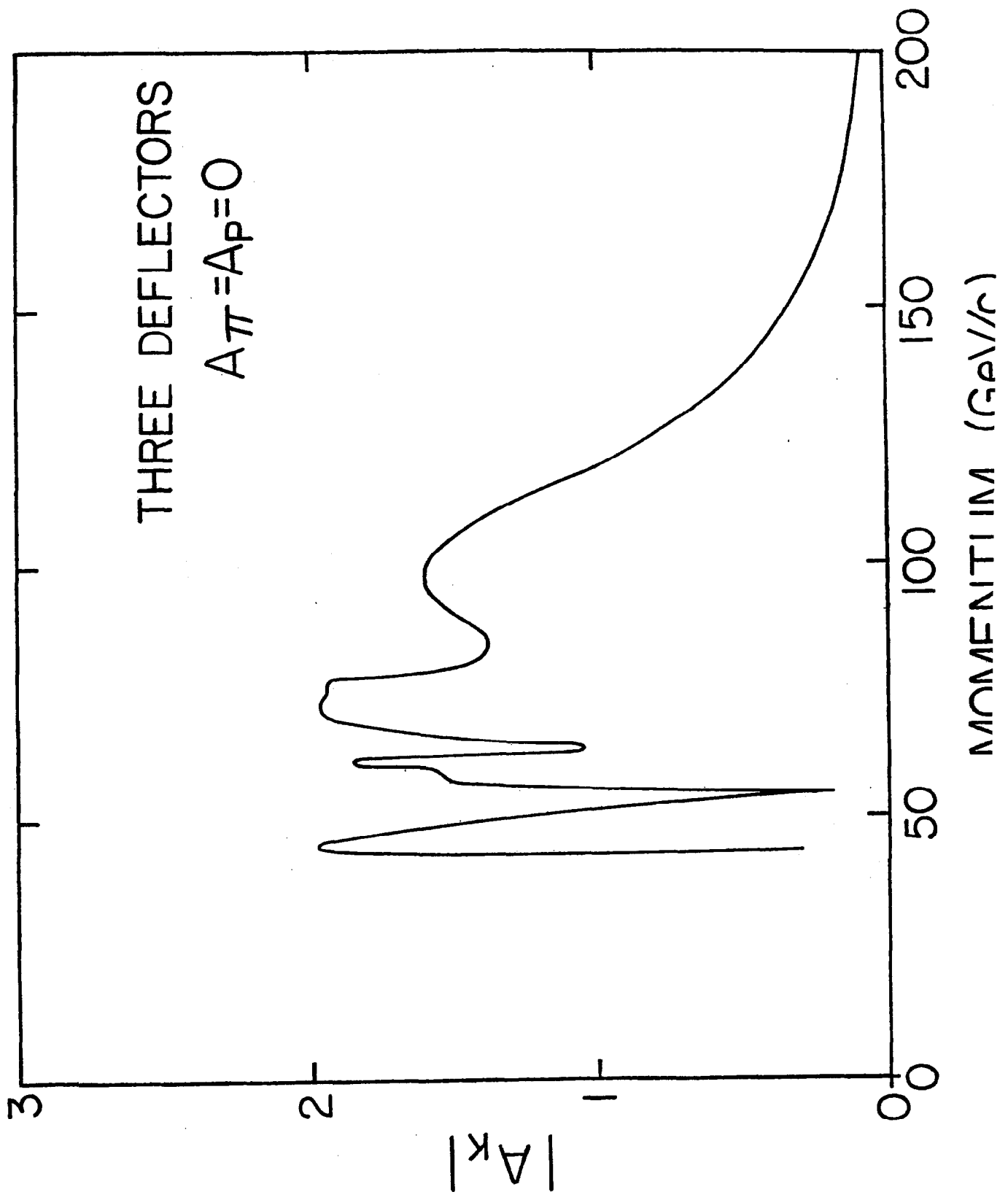
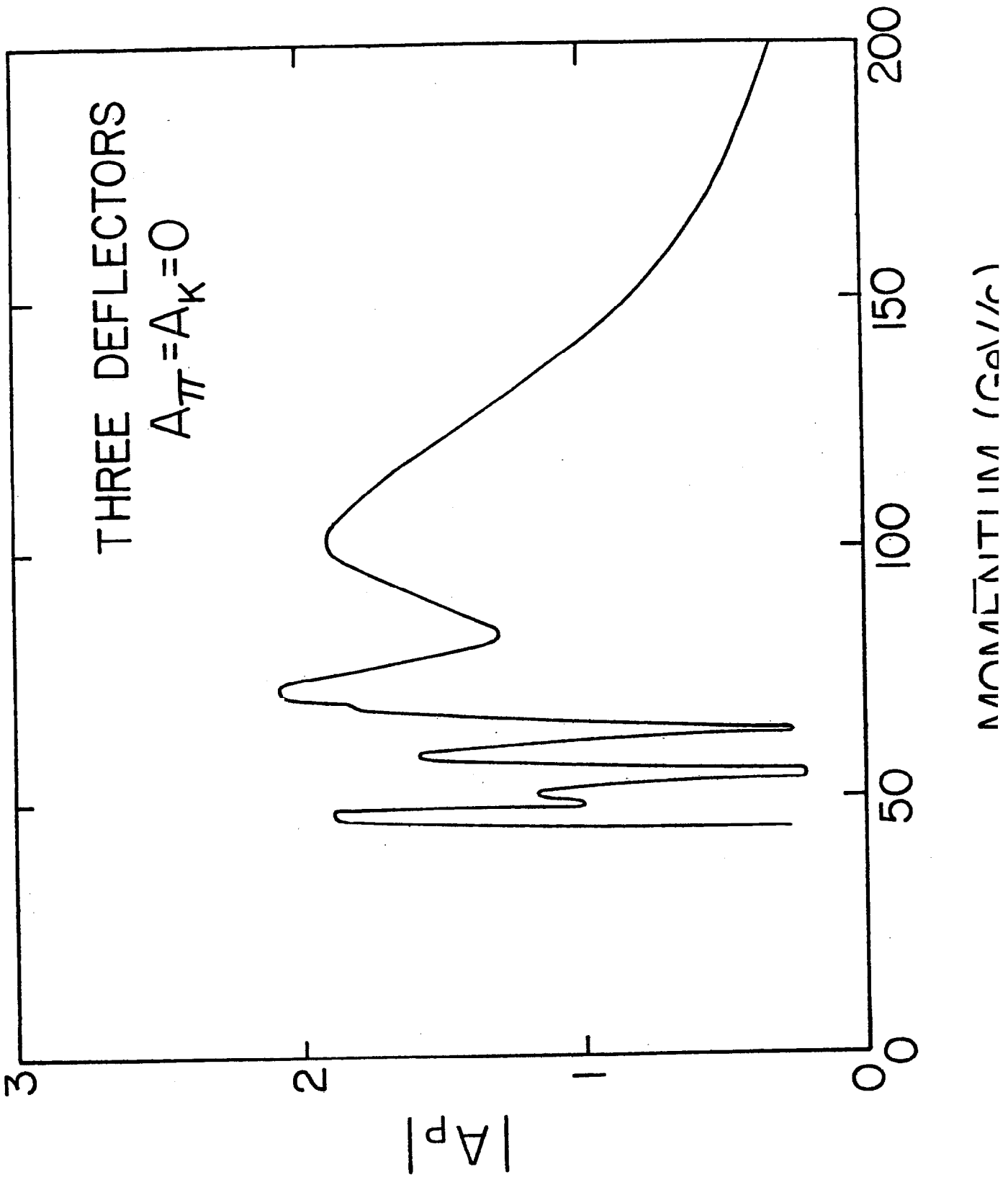


Figure 3

Figure 4







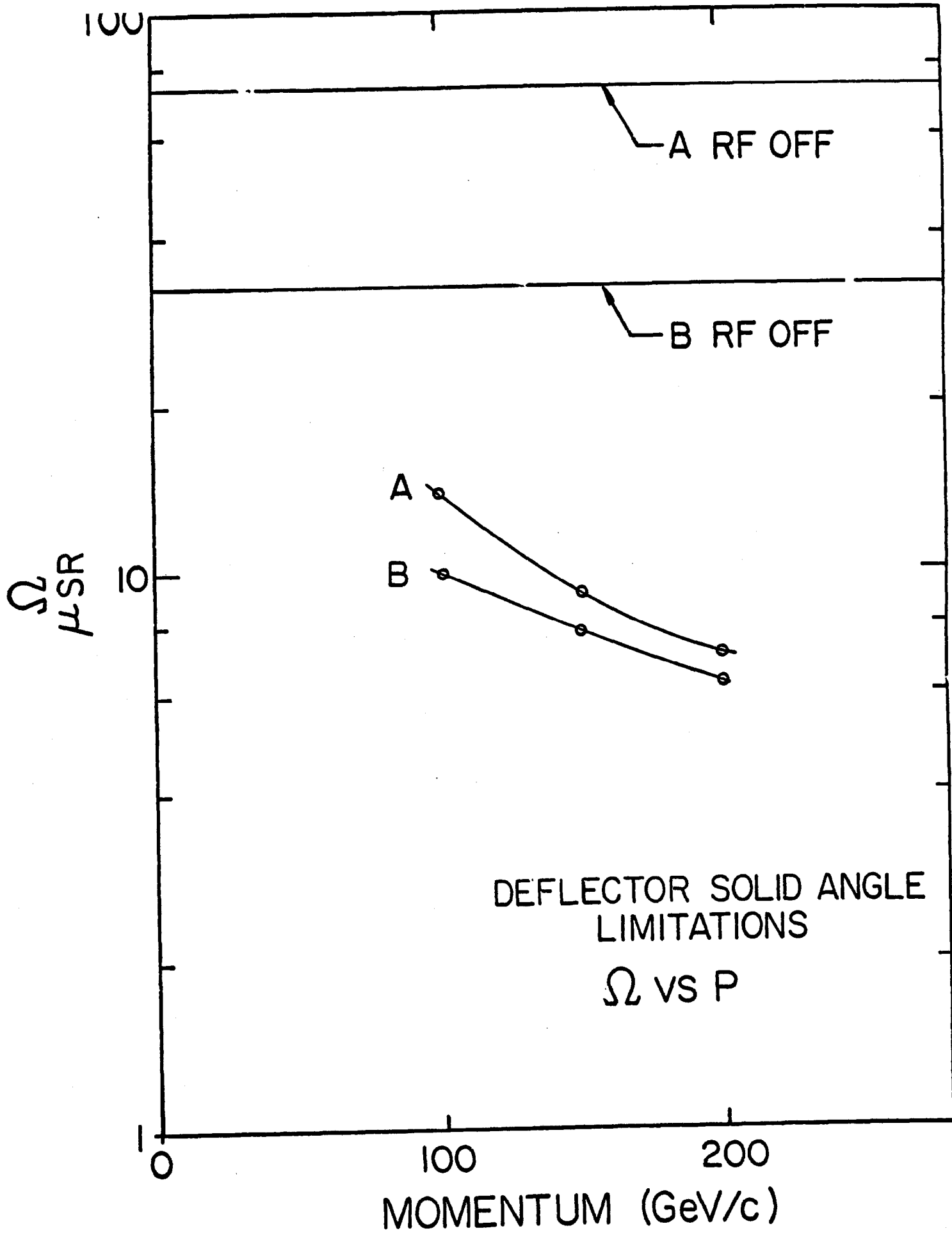


Figure 8

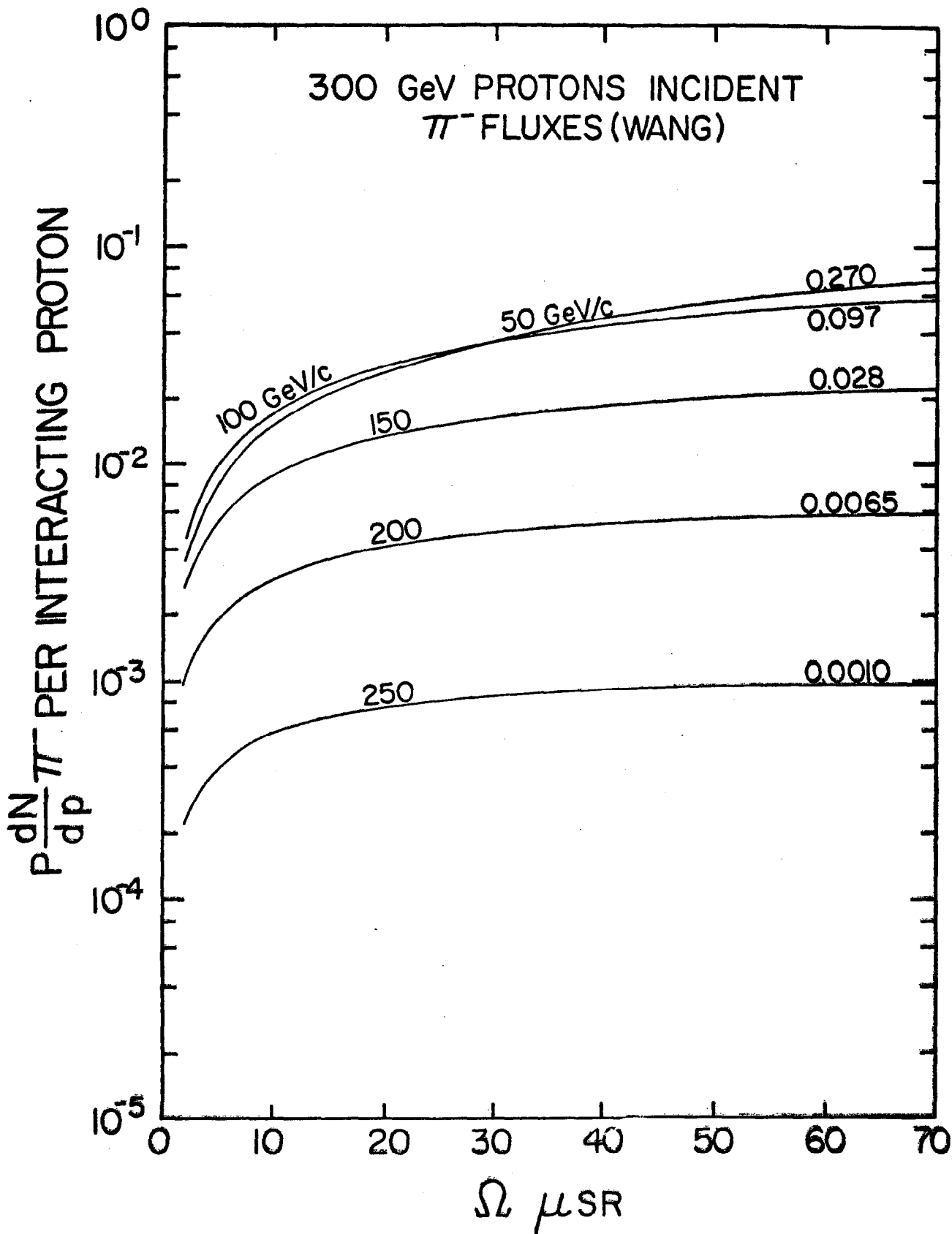


Figure 9

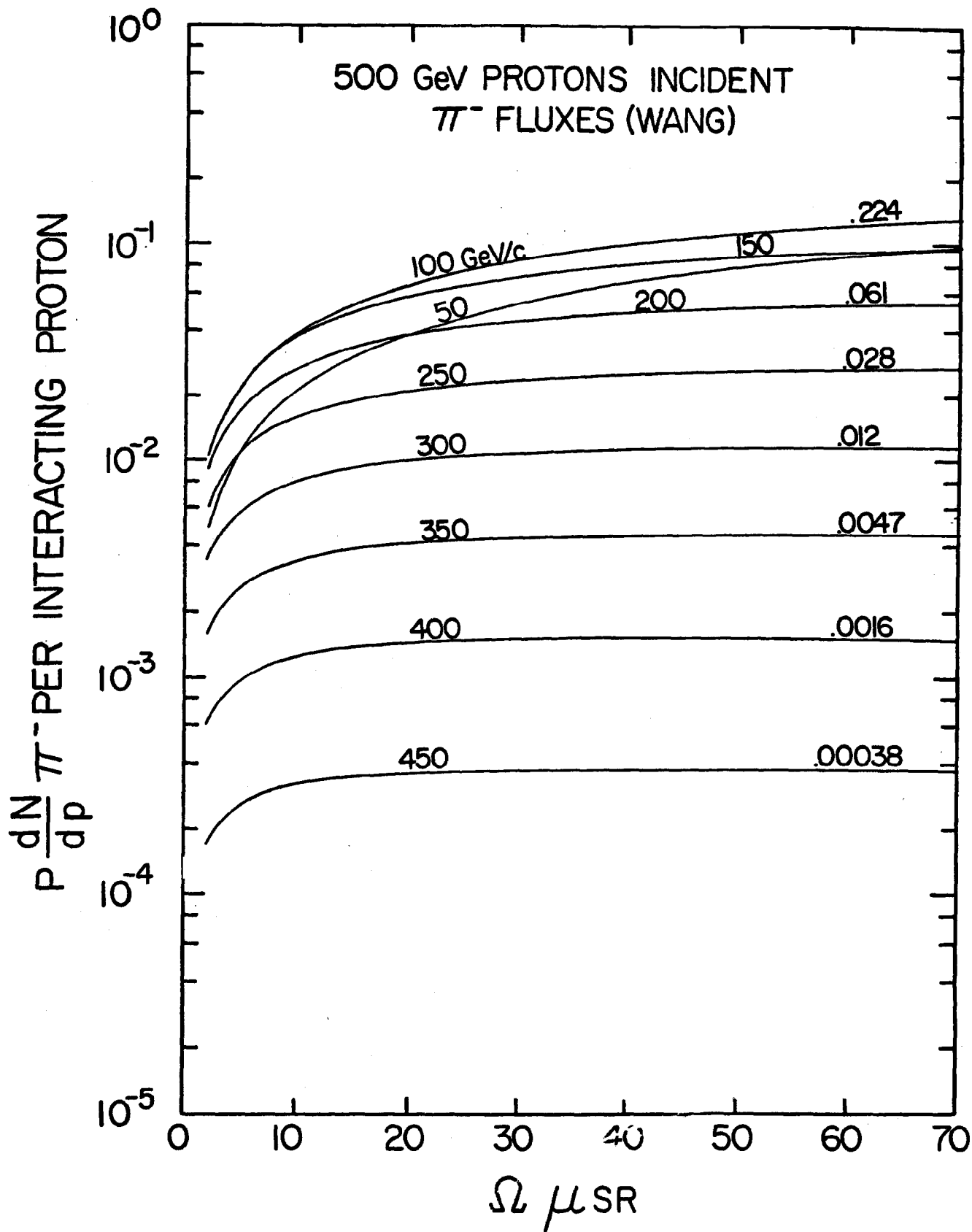


Figure 10

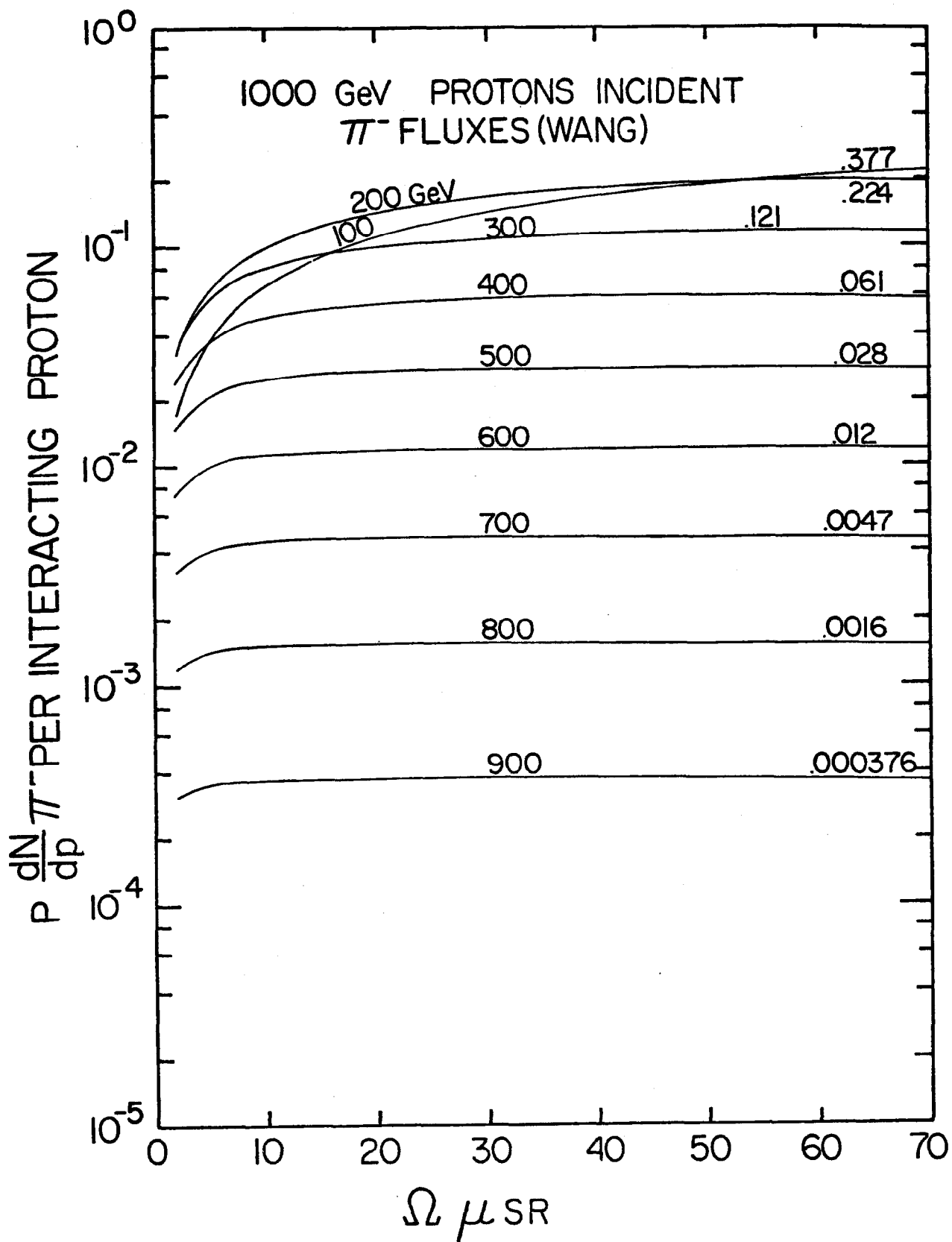


Figure 11

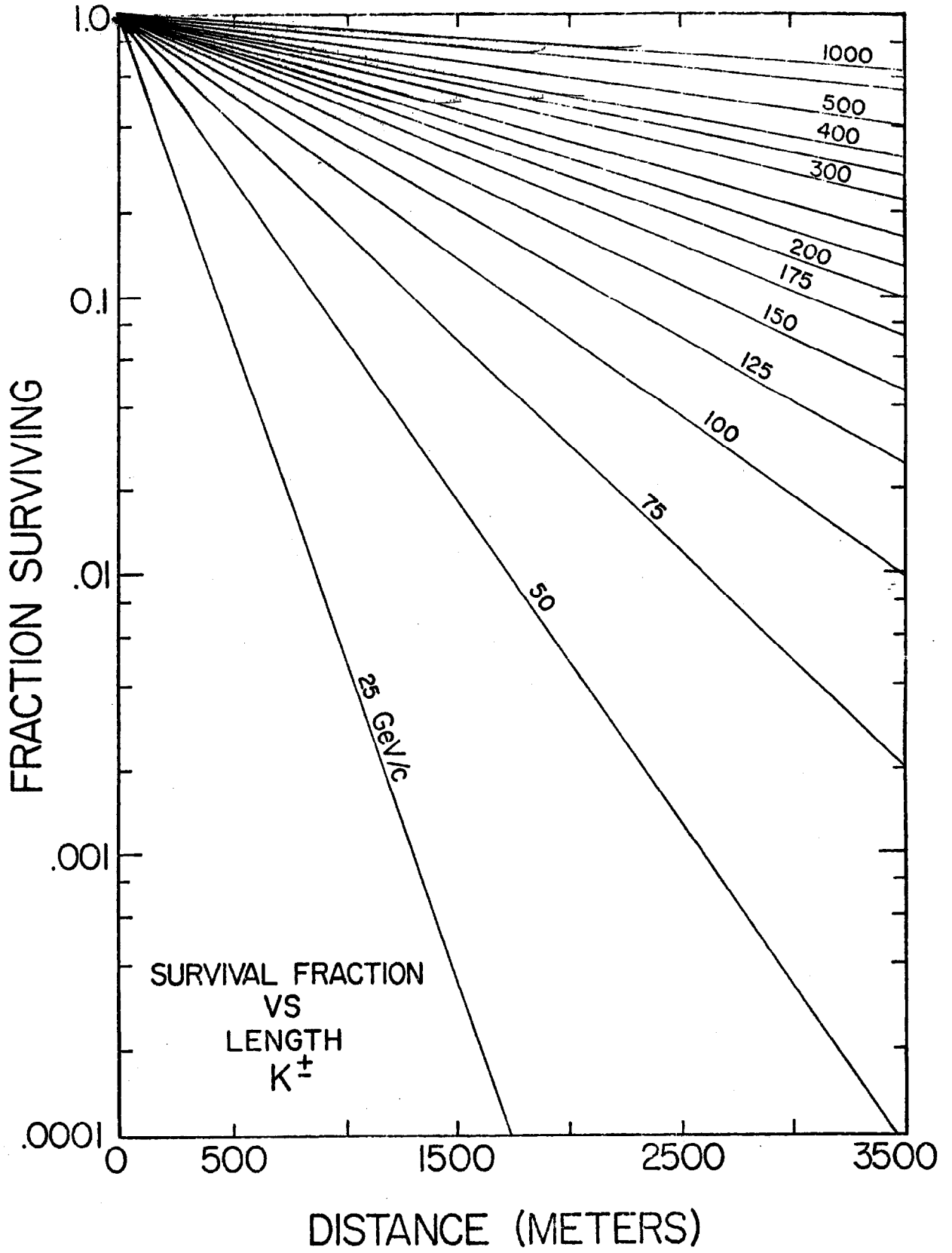


Figure 12

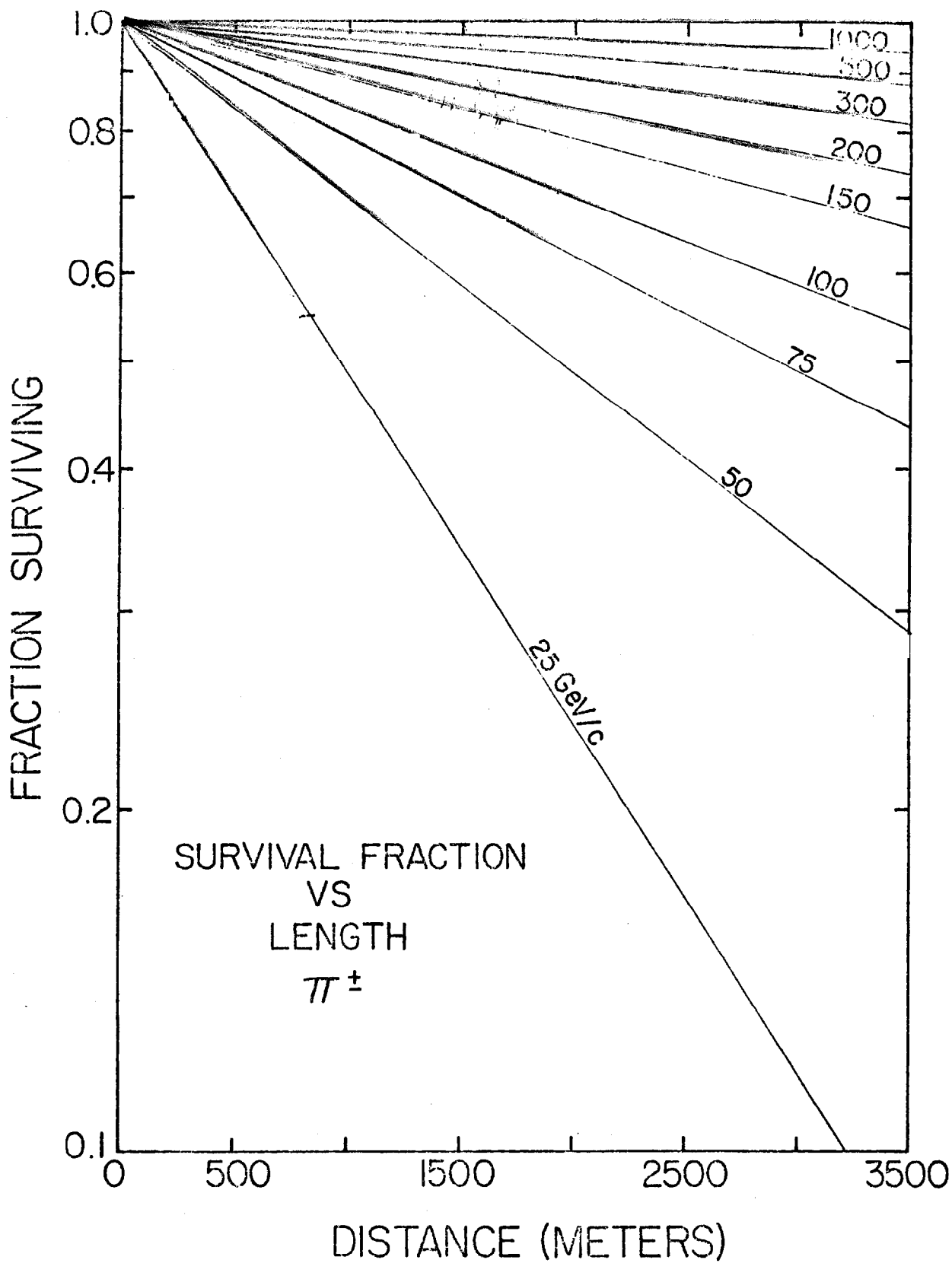


Figure 13

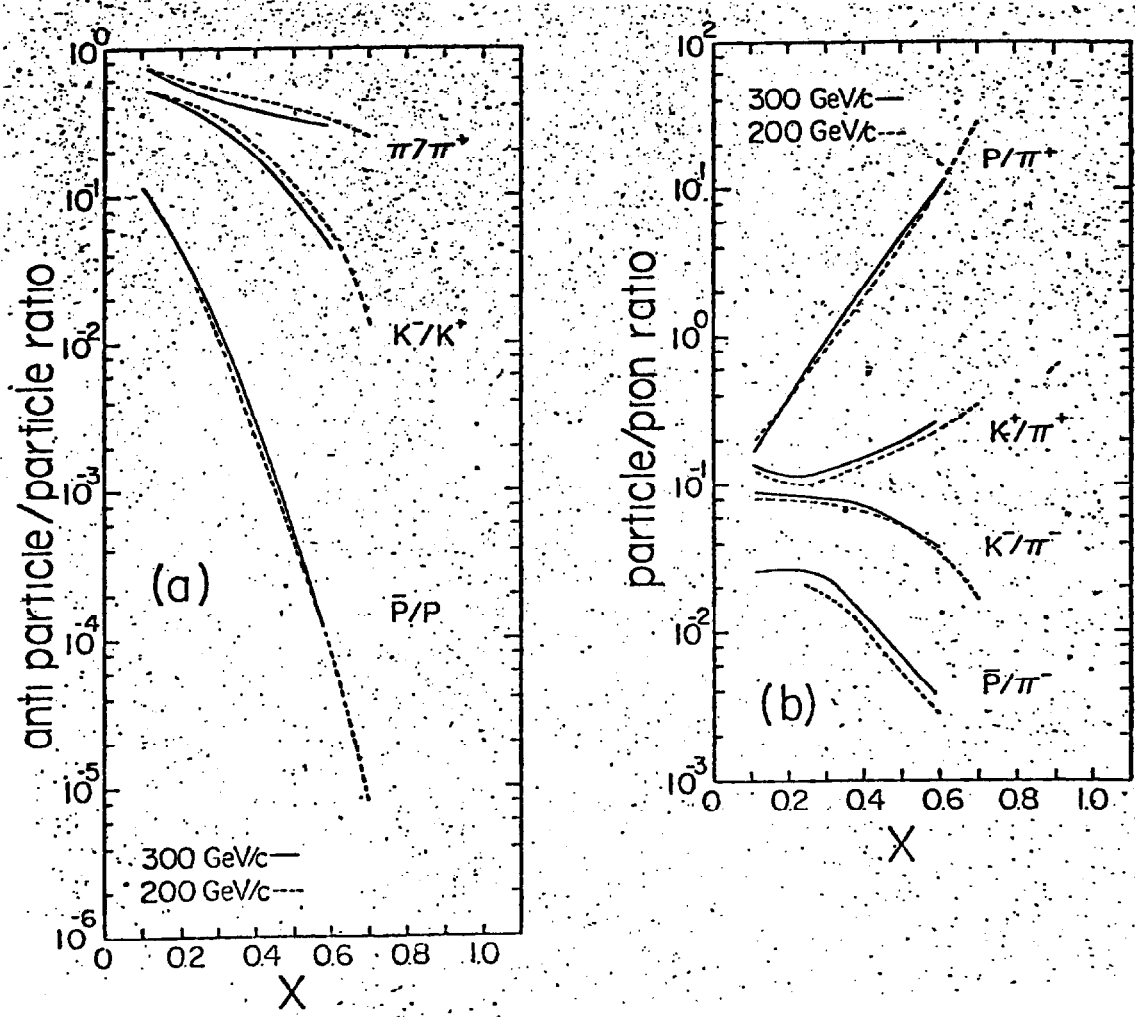


Figure 14

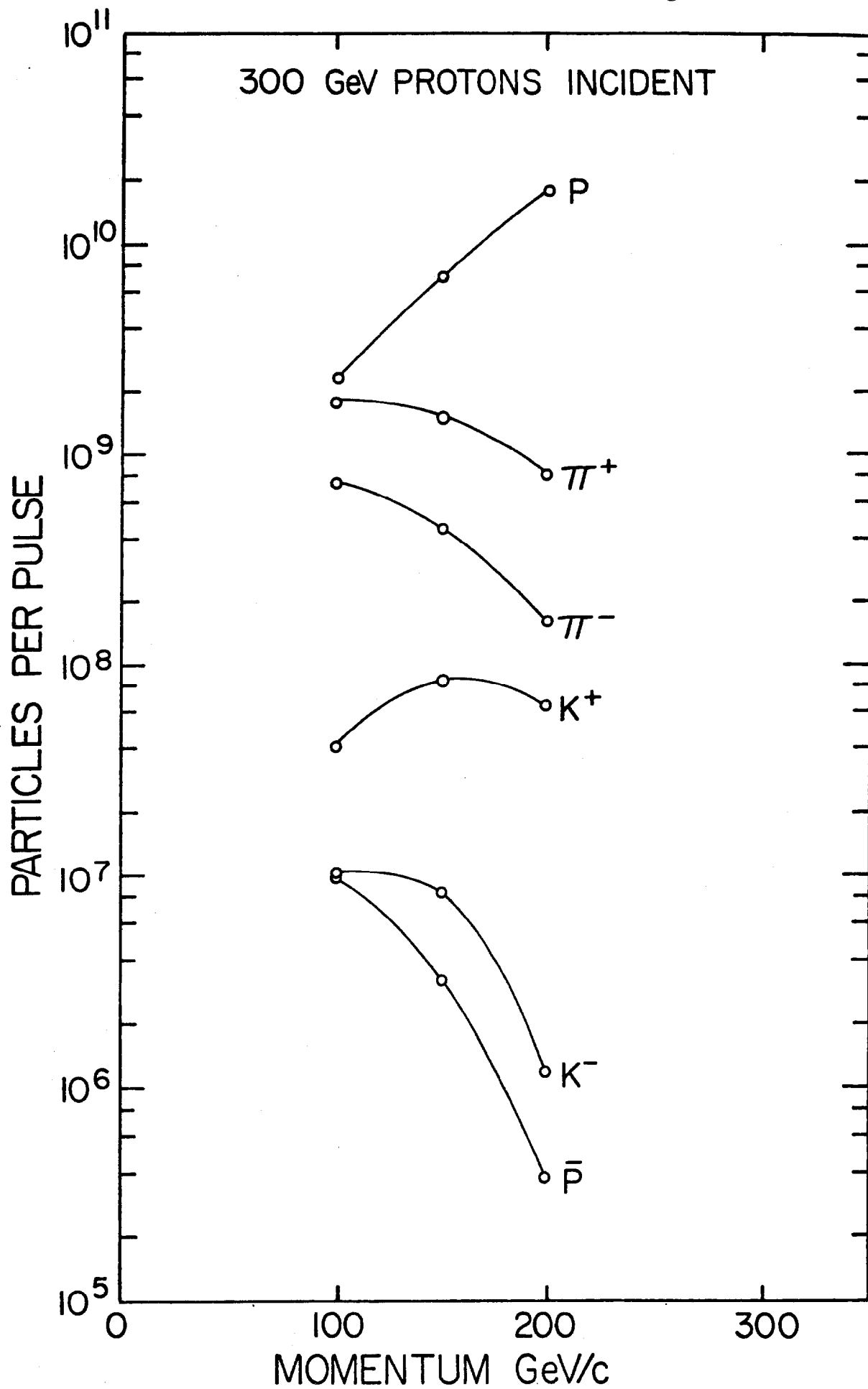


Figure 15

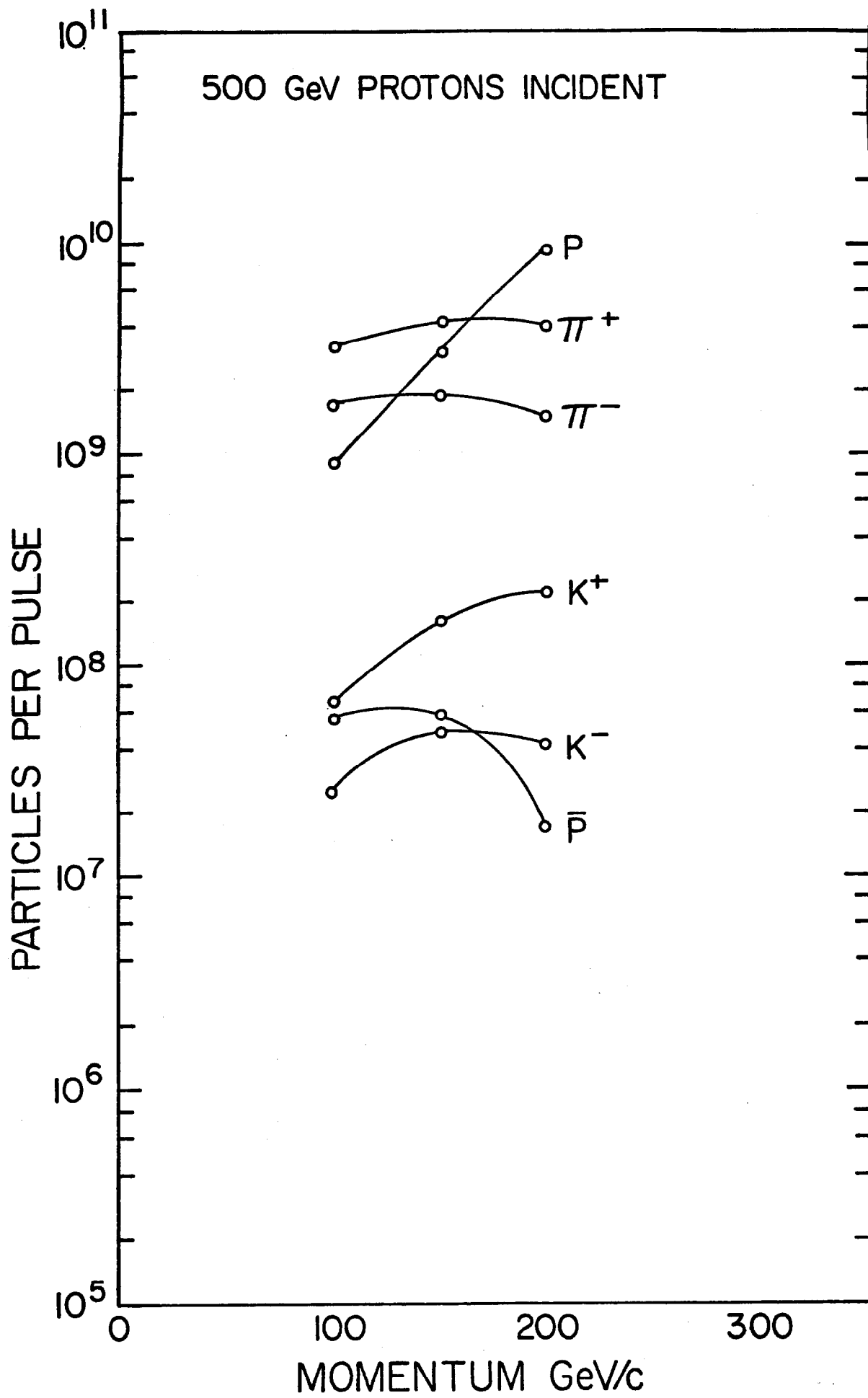


Figure 16

